Original Article
Mol Imaging Radionucl Ther 2023;32:123-130 DOI:10.4274/mirt.galenos.2022.08860

Potential Role of Somatostatin Receptor Scintigraphy for *In Vivo* Imaging of Vulnerable Atherosclerotic Plaques and Its Association with Myocardial Perfusion Imaging Finding: A Preliminary Study

Hassas Aterosklerotik Plakların İn Vivo Görüntülenmesinde Somatostatin Reseptör Sintigrafisinin Potansiyel Rolü ve Bunun Miyokardiyal Perfüzyon Görüntüleme Bulgusu ile İlişkisi: Bir Ön Çalışma

Abdullatif Amini[1], Esmail Jafari[2], Mohammad Reza Pourbehi[1], Dariush Iranpour[1], Reza Nemati[3], Hojjat Ahmadzadehfar[4], Majid Assadi[2]

[1]Bushehr University of Medical Sciences Faculty of Medicine, Bushehr Medical Heart Center, Bushehr, Iran
[2]The Persian Gulf Nuclear Medicine Research Center, Bushehr Medical University Hospital, School of Medicine, Bushehr University of Medical Sciences, Department of Molecular Imaging and Theranostics, Bushehr, Iran
[3]Bushehr University of Medical Sciences, Bushehr Medical University Hospital, Department of Neurology, Bushehr, Iran
[4]Klinikum Westfalen, Department of Nuclear Medicine, Dortmund, Germany

Abstract

Objectives: This study was conducted to detect atherosclerotic plaques with somatostatin receptor scintigraphy (SRS) using Tc-99m-octreotide that binds to somatostatin receptor-2.

Methods: Of the 783 patients referred for myocardial perfusion imaging (MPI), 52 underwent additional chest single-photon emission computed tomography (SPECT) with Tc-99m-octreotide and participated in this study. In addition, 43 patients who underwent Tc-99m-octreotide scan for neuroendocrine tumor (NET) also received cardiac SPECT. Angiography was performed within 1 month after SRS for 19 patients who showed intensive uptake in SRS and had cardiac risk factors.

Results: Of 52 patients who underwent MPI and SRS, 15 showed intensive cardiac uptake in SRS. Moreover, of 43 patients who were referred for NET, 4 patients had marked cardiac uptake in SRS in the heart. Nineteen patients including 12 women and 7 men aged 28 to 84 (58±8.04) years underwent coronary angiography. SRS and angiography in the left anterior descending territory were concordant in 15/19 (79%) patients, whereas only 7/15 (46%) cases had concordant MPI and angiography results. In the right coronary artery territory, SRS and angiography were concordant in 16/19 (84%) cases, while MPI and angiography were concordant in 11/15 (73%) cases. In the left circumflex artery territory, SRS and angiography were concordant in 15/19 (79%) cases, whereas MPI and angiography were concordant in 6/15 (40%) cases. In the remaining 76 patients who did not undergo coronary angiography based on cardiovascular profile and SRS, no cardiac events occurred in a follow-up of 2-11 months (7.52±2.71).

Conclusion: Tc-99m-octreotide uptake was more concordant with coronary plaques relative to MPI findings, suggesting a potential role for Tc-99m-octreotide in the evaluation of atherosclerosis.

Keywords: Tc-99m-octreotide, somatostatin receptor-2 (SSTR-2), myocardial perfusion scintigraphy, coronary angiography

Address for Correspondence: Prof. Majid Assadi, MD, FASNC, The Persian Gulf Nuclear Medicine Research Center, Bushehr Medical University Hospital, School of Medicine, Bushehr University of Medical Sciences, Department of Molecular Imaging and Theranostics, Bushehr, Iran
Phone: +0098-771-2580169 **E-mail:** asadi@bpums.ac.ir, assadipoya@yahoo.com ORCID ID: orcid.org/0000-0002-2166-3765
Received: 02.05.2022 **Accepted:** 15.08.2022

Öz

Amaç: Bu çalışma, somatostatin reseptör-2'ye bağlanan Tc-99m-oktreotid kullanılarak somatostatin reseptör sintigrafisi (SRS) ile aterosklerotik plakların saptanması amacıyla yapılmıştır.

Yöntem: Miyokardiyal perfüzyon görüntülemesi (MPI) için sevk edilen 783 hastadan 52'sine ek olarak Tc-99m-oktreotid ile göğüs tek foton emisyonlu bilgisayarlı tomografisi (SPECT) uygulandı ve bu hastalar çalışmaya katıldı. Ayrıca, nöroendokrin tümör (NET) için Tc-99m-oktreotid taraması yapılan 43 hastaya da kardiyak SPECT uygulandı. SRS'de yoğun tutulum gösteren ve kardiyak risk faktörü taşıyan 19 hastaya SRS'den sonraki 1 ay içinde anjiyografi yapıldı.

Bulgular: MPI ve SRS uygulanan 52 hastanın 15'inde SRS'de yoğun kardiyak tutulum görüldü. Ayrıca NET için yönlendirilen 43 hastanın 4'ünde kalpte SRS'de belirgin kardiyak tutulum saptandı. Yaşları 28 ile 84 (58±8,04) arasında değişen 12'si kadın, 7'si erkek olmak üzere 19 hastaya koroner anjiyografi yapıldı. SRS ve sol ön inen arter bölgesinde anjiyografi 15/19 (%79) hastada uyumlu iken, sadece 7/15 (%46) hastada uyumlu MPI ve anjiyografi sonuçları vardı. Sağ koroner arter bölgesinde 16/19 (%84) hastada SRS ve anjiyografi, 11/15 (%73) hastada MPI ve anjiyografi uyumluydu. Sol sirkumfleks arter bölgesinde 15/19 (%79) hastada SRS ve anjiyografi, 6/15 (%40) hastada MPI ve anjiyografi uyumluydu. Kardiyovasküler profil ve SRS'ye göre koroner anjiyografi yapılmayan geri kalan 76 hastada 2-11 aylık takipte (7,52±2,71) kardiyak olay gelişmedi.

Sonuç: Miyokardiyal perfüzyon görüntülemesi bulgularına göre Tc-99m-oktreotid alımının koroner plaklarla daha uyumlu olması, aterosklerozun değerlendirilmesinde Tc-99m-oktreotidin potansiyel bir rolü olduğunu düşündürmektedir.

Anahtar kelimeler: Tc-99m-oktreotid, somatostatin reseptör-2 (SSTR-2), miyokardiyal perfüzyon sintigrafisi, koroner anjiyografi

Introduction

Cardiovascular diseases are the main cause of about one-third of deaths in men and women across the world. It is estimated that more than 19 million patients worldwide suffer from cardiovascular disease annually. One common cause of cardiac events is the buildup of fats, cholesterol, and any other compounds in the arterial wall leading to the formation of plaques, known as vulnerable atherosclerotic plaques (VAPs) (1,2).

VAP formation in coronary arteries is one of the common causes of cardiac disease, which can lead to cardiac events and death. These plaques develop gradually and mild plaques usually have no complications. The complications of atherosclerosis start when the artery becomes occluded due to plaque formation, leading to inadequate blood supply to the tissues. A VAP may restrict coronary blood flow leading, leading myocardial infarction and death. A VAP consists of a fine fibrous cap and a vast lipid core, resulting in the accumulation of activated macrophages. The activated macrophages may rupture the VAP, resulting in sudden cardiac events and death. Given the importance of this issue, the detection of early changes in the coronary walls is of enormous importance (3,4). VAP, which is prone to rupture, usually does not cause marked stenosis; therefore, it is not diagnosed by myocardial perfusion imaging (MPI), the procedure commonly used for ischemia evaluation. Many preclinical and clinical studies have been conducted to understand VAP recently (5).

The standard methods for diagnosis of VAP include physical examination, laboratory tests, ankle/brachial index, electrocardiogram, and ultrasound examination, as well as invasive methods including intravascular coronary ultrasound, angiography, and angioscopy (6,7). All these procedures have differences in terms of sensitivity, specificity, availability, and reproducibility. Nowadays, molecular and cellular imaging has made it possible to evaluate early changes in the arterial walls toward VAP formation, opening new windows in detecting VAP in subclinical and clinical stages.

As mentioned earlier, VAPs result in the accumulation of activated macrophages, therefore imaging macrophages can be used as a potential target for the characterization and diagnosis of VAP. It has been indicated that somatostatin receptor-2 (SSTR-2) is overexpressed by activated macrophages (8). Several radiotracers have an affinity for somatostatin receptors, including SSTR-2, and are used for imaging and management of patients with neuroendocrine tumors (NETs) in multiple centers around the world, such as ^{68}Ga-DOTATATE positron emission tomography (PET) and Tc-99m-octreotide single-photon emission computed tomography (SPECT) (9,10,11,12).

The potential role of several radiotracers such as ^{68}Ga-DOTATATE and ^{18}F sodium florine PET in the evaluation of inflammatory processes and detection of VAP has been investigated in several studies (4,13,14,15,16). Therefore, this study was conducted to detect atherosclerotic plaques by somatostatin receptor scintigraphy (SRS) using Tc-99m-octreotide SPECT and to compare SRS with coronary angiography for detection of atherosclerotic plaques and its association with MPI using Tc-99m-MIBI SPECT finding.

Materials and Methods

Study Population

In this study, VAP was evaluated using Tc-99m-octreotide SPECT in the following patients at Bushehr Nuclear Medicine Department:

1. Patients who were referred for MPI were asked to perform an additional Tc-99m-octreotide SPECT for evaluation of VAP within 3 to 7 days following MPI.

2. Patients who were referred for evaluation of NETs by Tc-99m-octreotide and had cardiac risk factors underwent cardiac Tc-99m-octreotide SPECT in addition to the whole-body scan for evaluation of VAP (Figure 1).

A detailed history including age, hypertension, angina, diabetes, hyperlipidemia, smoking, family history of cardiac diseases, obesity and history of cardiac attack was taken from all patients for evaluation of cardiac risk factors. The inclusion criteria were age >18 and the presence of cardiac risk factors. In addition, because of the possibility of false-positive results, patients with a history of interventional coronary therapy such as CABG or stent were excluded from the study. The images were evaluated by nuclear medicine physicians. Patients who showed significant uptake of Tc-99m-octreotide in the heart and had cardiac risk factors were asked to undergo angiography for the evaluation of VAP in coronary arteries. This study was approved by a local ethics committee, and written consent was obtained from all patients before each stage of the study. The Ethical Committee of Bushehr University of Medical Sciences approved this study (IR.BPUMS.REC.1401.175).

Image Acquisition

SPECT Images

Patients fasted overnight and all cardiovascular medications were discontinued at least 2 days before the study. An intravenous line of normal saline solution was connected to the antecubital vein using a 20-gauge cannula. Dipyridamole (0.56 mg/kg) was infused above 4 min. Patients' symptoms and three-lead electrocardiography were monitored continuously. A dose of 740 MBq of Tc-99m-sestamibi as a compact bolus was injected 4 min after the initiation of the infusion. Sixty minutes later, the patients were asked to eat a fatty meal to accelerate hepatobiliary clearance of Tc-99m sestamibi, and imaging was performed 90 min after the initial infusion of dipyridamole. The rest phase was performed next day.

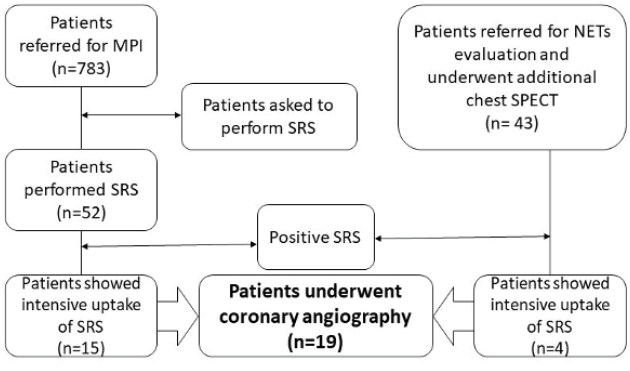

Figure 1. Study design
MPI: Myocardial perfusion imaging, SRS: Somatostatin receptor scintigraphy, NETs: Neuroendocrine tumors, SPECT: Single-photon emission computed tomography

The one-day stress-rest protocol was used for MPI. Patients fasted overnight and all cardiovascular drugs were stopped at least 2 days before the examination. In the stress phase, the patients underwent treadmill testing or pharmacologic stress with the infusion of 0.56 mg/kg dipyridamole over 5 min. Then 370-555 MBq (10-15 mCi) Tc-99m-sestamibi (ParsIsotope Co., Iran) was administered at the peak of stress. SPECT images were acquired 30-45 minutes after stress. Four hours after the stress phase, the rest phase was performed with an injection of 740-925 MBq (20-25 mCi) Tc-99m-sestamibi. SPECT images were acquired 60-90 minutes after the radiotracer injection.

For SRS, 60 to 90 min following injection of 740-925 MBq (20-25 mCi) Tc-99m-octreotide, SPECT imaging of the heart was performed in addition to a whole-body scan.

The scans were acquired using a dual-head gamma camera (ADAC-Pegasys) equipped with a low-energy high-resolution collimator, a 140 keV photopeak with a 20% energy window, and a matrix size of 64x64. The SPECT images were acquired with 32 projections (20 seconds/projection) 180° rotations from RAO to LPO for MPI and with 64 projections (20 seconds/projection) and 360° rotations for SRS. Image reconstruction was performed using the filtered back projection method (Wiener filter; cut-off: 0.66, order: 5). The images were evaluated by a nuclear medicine specialist.

Coronary Angiography

Angiography was performed using the standard Judkins method. A cardiologist who was not aware of the scintigraphic results analyzed the angiograms.

Image Analysis

In this study, a blinded cardiologist evaluated the angiographic data and a blinded nuclear medicine specialist evaluated the scintigraphic data. The coronary arteries are divided into three main arteries, including the left anterior descending (LAD), right coronary artery (RCA), and left circumflex artery (LCx), according to angiographic standards. In scintigraphic images, the left ventricular wall was mapped to the standard 17-segment model.

For MPI, a 17-segment model was used for interpretation. According to this model, the left ventricle was divided into three main coronary arteries. For the evaluation of each segment, changes in radiotracer uptake in stress and rest phases were evaluated. A decreased radiotracer uptake

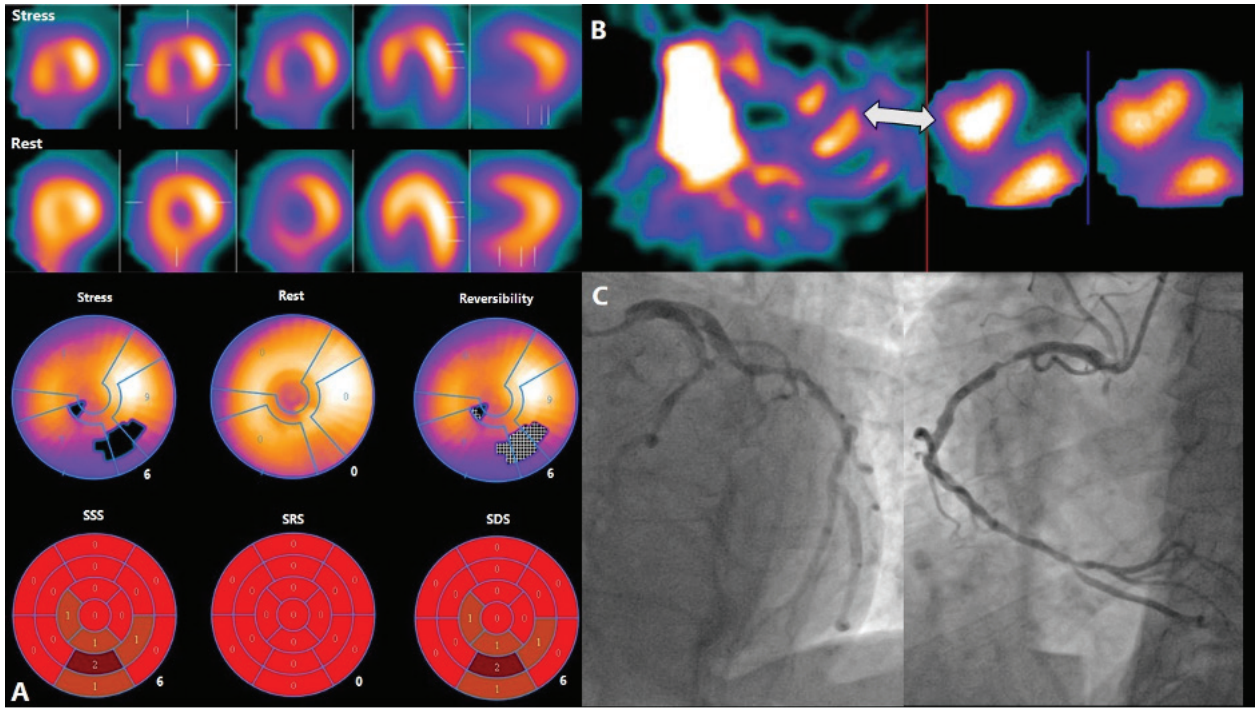

Figure 2. Myocardial perfusion imaging (MPI) single-photon emission computed tomography (SPECT) of a 64-year-old woman with non-specific chest symptoms who was referred from the department of cardiology for assessment of the perioperative risk of ischemic cardiac events. MPI SPECT showed only mild ischemia in the inferoseptal wall (A). Somatostatin receptor scintigraphy using Tc-99m-octreotide SPECT in the same patient showed intense uptake areas in the inferior and anterior regions (B). Coronary angiography showed a severe left anterior descending lesion just after the diagonal branch, cut-off diagonal branch, multiple non-significant plaques in the left circumflex, severe proximal right coronary artery lesion, and a severe lesion of the PDA origin (C)

(defect) observed in the stress phase that improved on rest was considered an ischemic defect, and a stress defect that did not improve was considered a fixed defect. In this study, any myocardial defect observed in the region of interest was considered abnormal.

For SRS, similar to MPI, the left ventricle was mapped into 17 segments and then divided into three main coronary arteries. For interpretation, any marked radiotracer uptake in these 17 regions as compared to background tissue was considered VAP in that region.

Statistical Analysis

Statistical analysis was performed using SPSS software version 21 for Windows. The continuous variables are expressed as median ± standard error of mean.

Results

Of 783 patients with suspected coronary artery disease who presented to Bushehr Nuclear Medicine Department for MPI, 52 consented to perform additional SRS and were included in the final study cohort. In addition, 43 patients who underwent Tc-99m-octreotide scan for NET also underwent cardiac SPECT. In total, 95 cases had cardiac Tc-99m-octreotide SPECT for evaluation of VAP. Of these 95 patients, 19 patients, including 12 women and 7 men aged 28 to 84 (58±8.04) years) who showed marked radiotracer uptake in SRS, underwent coronary angiography. An example of such a case is presented in Figure 2. Four out of 19 patients were NET patients who did not undergo MPI. Angiography was abnormal in all 19 patients, while MPI was normal in one of them. The baseline characteristics of the patients are shown in Table 1.

As for concordance between scintigraphic data and angiography in three main arteries, the results of SRS and angiography were concordant in the LAD territory in 15/19 (79%) patients, while only 7/15 (46%) cases had concordant MPI and angiography results. In the RCA territory, the results of SRS and angiography were concordant in 16/19 (84%) cases, while MPI and angiography results were concordant in 11/15 (73%) cases. In the LCx territory, the results of SRS and angiography were concordant in 15/19 (79%) cases, while MPI and angiography were concordant in 6/15 (40%) cases. Table 2 shows the results in detail. A false positive and false negative case is presented in Figure 3.

Table 1. Baseline characteristics of patients	
	Patients (n=19)
Age (mean ± SD)	58±8.04
Sex (female)	12 (63.2)
Chest pain	8 (42.1%)
Cardiac risk factor	
Hypertension	11 (57.9%)
Diabetes	9 (47.4)
Smoking	7 (36.8%)
Hyperlipidemia	8 (42.1%)
Family history	3 (15.8%)
Obesity	3 (15.8%)
Cardiac attack	3 (15.8%)
SD: Standard deviation	

As for the scintigraphic data, the results of SRS and MPI were concordant in 11/15 (73%), 10/15 (66%), and 10/15 (66%) patients in the LAD, RCA, and LCx territories, respectively (Table 3).

Cardiac events were not observed in a follow-up period of 2-11 months (7.52±2.71) in any of the remaining 76 patients who did not undergo coronary angiography based on the cardiovascular profile. Interestingly, they did not show a remarkable uptake on SRS.

Discussion

This study was conducted to evaluate coronary VAP using SRS and compare it with MPS and angiography for the first time. Several studies have evaluated PET radiotracers

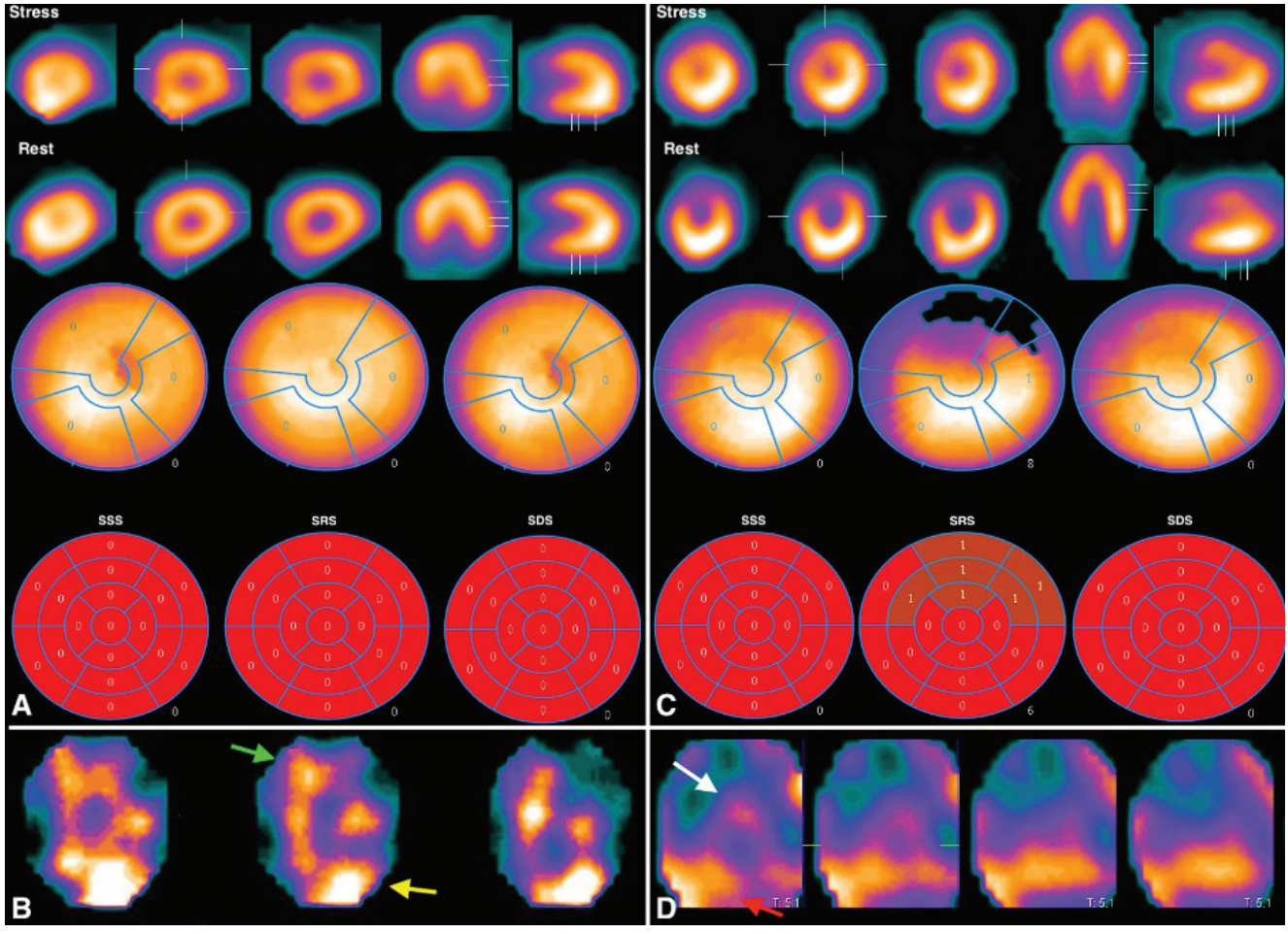

Figure 3. The cardiac examination of a 58-year-old woman presented with normal myocardial perfusion imaging (MPI) (A). Somatostatin receptor scintigraphy (SRS) single-photon emission computed tomography indicated uptake in anteroseptal [left anterior descending (LAD)] (green arrow) and inferior wall [right coronary artery (RCA)] (yellow arrow) (B) but angiography showed LAD lesion and normal RCA resulted in false positive in SRS, which may be due to liver uptake. In another case, cardiac examination of a 64-year-old woman presented with a defect in the anteroseptal wall according to MPI (C). In SRS, only uptake in the anterolateral wall (LAD) (white arrow) was reported and uptakes in the inferior and inferoseptal (RCA) (red arrow) were considered as liver uptake (D), but lesions were observed in both LAD and RCA in coronary angiography, which resulted in false negatives, which may be due to liver uptake

Table 2. Concordance between coronary angiography and SRS and MPI

		Angiography								
		LAD			RCA			LCx		
		Negative	Positive	Concordance	Negative	Positive	Concordance	Negative	Positive	Concordance
SRS	Negative	4	3	15/19 (79%)	5	2	16/19 (84%)	7	0	15/19 (79%)
	Positive	1	11		1	11		4	8	
MPI	Negative	3	7	7/15 (46%)	4	4	11/15 (73%)	4	4	6/15 (40%)
	Positive	1	4		0	7		5	2	

SRS: Somatostatin receptor scintigraphy, MPI: Myocardial perfusion imaging, LAD: Left anterior descending, RCA: Right coronary artery, LCx: Left circumflex artery

Table 3. Concordance between SRS and MPI

		SRS								
		LAD			RCA			LCx		
		Negative	Positive	Concordance	Negative	Positive	Concordance	Negative	Positive	Concordance
MPI	Negative	6	0	11/15 (73%)	4	4	10/15 (66%)	4	4	10/15 (66%)
	Positive	4	5		1	6		1	6	

MPI: Myocardial perfusion imaging, SRS: Somatostatin receptor scintigraphy, LAD: Left anterior descending, RCA: Right coronary artery, LCx: Left circumflex artery

such as ^{68}Ga-DOTATATE, ^{18}F-fluorodeoxyglucos (FDG), and ^{18}F sodium florine for VAP (4,7,15,16,17); however, no study has investigated SPECT radiotracers. We previously reported the role of SRS in a case of myocarditis (18).

It has been shown that about 50% of cardiovascular-related mortality is due to acute myocardial infarction. About 75% of myocardial infarctions are due to an acute thrombotic event because of the rupture of a VAP, and plaque erosion is responsible for the remaining 25% (19). Because of the importance of this subject, early detection of VAP is of great significance.

Clinically, according to the guidelines (20,21), invasive coronary angiography is considered the gold standard investigation in patients presenting with symptoms of CAD and angina. MPI is performed when the diagnosis is equivocal or to evaluate the functional significance of a familiar coronary lesion. CT coronary angiography (CTa) is another modality that may help to avoid invasive methods. Except for CTa, other above-mentioned modalities are only used for detection of obstructive intraluminal stenosis and therefore provide little information on the nature of plaques and cannon determine the vulnerability of plaques (22). It has been shown that multicontrast magnetic resonance imaging (MRI) has the highest potential for evaluation of carotid plaque and interrogation of the fibrous cap, but its high cost and lengthy procedure are its major limitations (23,24).

Molecular imaging procedures have attracted attention for the evaluation of VAP, which provide additional information about the process of VAP formation such as calcification, apoptosis, hypoxia, and neovascularization as a non-invasive method. Moreover, these procedures can lead to early diagnosis of high-risk patients with prospective culprit lesions and help to prevent subsequent cardiovascular events with proper management (22). Clinically, many studies have investigated two molecular imaging protocols including ultrasmall superparamagnetic iron oxide-contrast-enhanced MRI and ^{18}F-FDG-PET (25). Although ^{18}F-FDG-PET is the most common radiotracer for nuclear plaque imaging, some other PET radiotracers, including 11C and ^{18}F-choline, 11C-PK11195, 11C-acetate, ^{18}F-sodium fluoride, and ^{68}Ga-DOTATATE, have also been studied for plaque imaging (4,13,14).

Biologically, VAP formation occurs following endothelial injury and accumulation of low-density lipoprotein cholesterol in the intimal layer of the coronary wall. Monocytes are recruited into the damaged wall in response to damage and transform into macrophages (26). This inflammatory process following the accumulation of activated macrophages on the coronary wall can lead to destabilization, progression, initiation, and finally rupture of the VAP, which causes the cardiac event. Therefore, this inflammatory process can be used for imaging and diagnosis of VAP (17).

Because of the overexpression of SSTR-2 on activated macrophages, ^{68}Ga-DOTATATE PET and Tc-99m-octreotide, which have a high affinity for SSTR-2 and an unremarkable uptake in the normal myocardium, can be used for the evaluation of VAP. The role of ^{68}Ga-DOTATATE in the evaluation of VAP has been demonstrated in several

studies. Rominger et al. (13) studied the uptake of ^{68}Ga-DOTATATE in the LAD and showed a significantly increased ^{68}Ga-DOTATATE uptake in the LAD, suggesting the potential role of this tracer for plaque imaging in the coronary arteries. Mojtahedi et al. (4) evaluated the uptake of ^{68}Ga-DOTATATE in the coronary arteries for the detection of VAP. They reported a significantly increased uptake in fibrotic and VAPs compared with normal coronary arteries (4). In addition, previous studies have shown the superiority of ^{68}Ga-DOTATATE for detecting VAP compared to ^{18}F-FDG (14,17).

In this study, all patients with significant uptake of the radiotracer in SRS had abnormal coronary angiography. The results showed a high concordance between SRS and coronary angiography in three main coronary arteries; therefore, SRS can be used as a non-invasive and widely available modality for the assessment of VAP. The higher concordance of SRS with coronary angiography compared to MPI may be due to the inability of MPI to detect plaques without remarkable coronary stenosis, which can be detected by SRS. Therefore, early VAPs can be detected using SRS, which prevents future cardiac events. In conclusion, SRS and MPI complete each other in the assessment of coronary artery diseases.

Finally, it should be mentioned that PET radiotracers, including ^{68}Ga-DOTATATE and ^{18}F-FDG, are the best radiotracers for nuclear plaque imaging because in comparison between PET and SPECT, PET has a higher spatial resolution and sensitivity. Moreover, absolute quantification of radionuclide uptake can be performed by PET. However, SPECT has advantages that cannot be ignored including lower costs, wider availability, and better physical properties of its radionuclides such as longer half-life. Therefore, the SPECT protocol is more applicable than PET for evaluating VAP, especially in regions where PET is less available.

Study Limitations

The limitations of this study include its small sample size and lack of PET/CT and SPECT/CT for anatomical assessment. Therefore, studies with larger populations are warranted for the validation of the clinical use of SPECT with somatostatin receptor imaging for evaluating VAP. In addition, due to ethical considerations, coronary angiography was only performed for patients according to cardiovascular guidelines, which may limit the accuracy of the findings due to the lack of angiography results in all SRS participants. It is necessary to perform accurate diagnostic tests, e.g. IVUS, accompanied by histological examinations for all patients undergoing SRS to improve the results. Another limitation of the study is that not all ischemic lesions diagnosed on MPI are due to plaque formation in the coronary arteries; therefore, plaque detection is not a good measure for comparing these two tests. Further well-designed studies are required to verify these preliminary findings.

Conclusion

The results of Tc-99m-octreotide uptake were more concordant with coronary plaques than Tc-99m-MIBI SPECT, suggesting a potential role for Tc-99m-octreotide in the evaluation of atherosclerosis. In addition, coronary uptake may provide a molecular guide for coronary atherosclerotic lesions. Specific regional uptake should be ascertained by histology.

Ethics

Ethics Committee Approval: The Ethical Committee of Bushehr University of Medical Sciences approved this study (IR.BPUMS.REC.1401.175).

Informed Consent: All participants provided written informed consent before participation

Peer-review: Externally and internally peer-reviewed.

Authorship Contributions

Surgical and Medical Practices: A.A., M.R.P., D.I., H.A., M.A., Concept: A.A., M.R.P., R.N., H.A., M.A., Design: E.J., D.I., R.N., H.A., M.A., Data Collection or Processing: A.A., E.J., M.R.P., D.I., H.A., M.A., Analysis or Interpretation: E.J., R.N., H.A., M.A., Literature Search: E.J., Writing: E.J., H.A., M.A.

Conflict of Interest: No conflict of interest was declared by the authors.

Financial Disclosure: The authors declared that this study has received no financial support.

References

1. Lambert MA, Weir-McCall JR, Salsano M, Gandy SJ, Levin D, Cavin I, Littleford R, MacFarlane JA, Matthew SZ, Nicholas RS, Struthers AD, Sullivan F, Henderson SA, White RD, Belch JJF, Houston JG. Prevalence and distribution of atherosclerosis in a low- to intermediate-risk population: assessment with whole-body MR angiography. Radiology 2018;287:795-804.
2. Ghanem AM, Hamimi AH, Matta JR, Carass A, Elgarf RM, Gharib AM, Abd-Elmoniem KZ. Automatic coronary wall and atherosclerotic plaque segmentation from 3D coronary CT angiography. Sci Rep 2019;9:47.
3. Bentzon JF, Otsuka F, Virmani R, Falk E. Mechanisms of plaque formation and rupture. Circ Res 2014;114:1852-1866.
4. Mojtahedi A, Alavi A, Thamake S, Amerinia R, Ranganathan D, Tworowska I, Delpassand ES. Assessment of vulnerable atherosclerotic and fibrotic plaques in coronary arteries using (68)Ga-DOTATATE PET/CT. Am J Nucl Med Mol Imaging 2015;5:65-71.
5. Dickson BC, Gotlieb AI. Towards understanding acute destabilization of vulnerable atherosclerotic plaques. Cardiovasc Pathol 2003;12:237-248.

6. Gallino A, Stuber M, Crea F, Falk E, Corti R, Lekakis J, Schwitter J, Camici P, Gaemperli O, Di Valentino M, Prior J, Garcia-Garcia HM, Vlachopoulos C, Cosentino F, Windecker S, Pedrazzini G, Conti R, Mach F, De Caterina R, Libby P. "In vivo" imaging of atherosclerosis. Atherosclerosis 2012;224:25-36.
7. Malmberg C, Ripa RS, Johnbeck CB, Knigge U, Langer SW, Mortensen J, Oturai P, Loft A, Hag AM, Kjær A. 64Cu-DOTATATE for noninvasive assessment of atherosclerosis in large arteries and its correlation with risk factors: head-to-head comparison with 68Ga-DOTATOC in 60 patients. J Nucl Med 2015;56:1895-1900.
8. Armani C, Catalani E, Balbarini A, Bagnoli P, Cervia D. Expression, pharmacology, and functional role of somatostatin receptor subtypes 1 and 2 in human macrophages. J Leukoc Biol 2007;81:845-855.
9. Al Bulushi N, Al Suqri B, Al Aamri M, Al Hadidi A, Al Jahdami H, Al Zadjali M, Al Risi M. Diagnostic accuracy of technetium-99m-octreotide in imaging neuroendocrine tumors, Oman hospital experience with literature review. World J Nucl Med 2019;18:137-142.
10. Pirayesh E, Amoui M, Assadi M. Uptake difference by somatostatin receptors in a patient with neuroendocrine tumor: 99mTc-octreotide uptake in the lung without uptake in liver lesions. Mol Imaging Radionucl Ther 2015;24:128-131.
11. H Haug AR, Cindea-Drimus R, Auernhammer CJ, Reincke M, Wängler B, Uebleis C, Schmidt GP, Göke B, Bartenstein P, Hacker M. The role of 68Ga-DOTATATE PET/CT in suspected neuroendocrine tumors. J Nucl Med 2012;53:1686-1692.
12. Haug AR, Cindea-Drimus R, Auernhammer CJ, Reincke M, Beuschlein F, Wängler B, Uebleis C, Schmidt GP, Spitzweg C, Bartenstein P, Hacker M. Neuroendocrine tumor recurrence: diagnosis with 68Ga-DOTATATE PET/CT. Radiology 2014;270:517-525.
13. Rominger A, Saam T, Vogl E, Ubleis C, la Fougère C, Förster S, Haug A, Cumming P, Reiser MF, Nikolaou K, Bartenstein P, Hacker M. In vivo imaging of macrophage activity in the coronary arteries using 68Ga-DOTATATE PET/CT: correlation with coronary calcium burden and risk factors. J Nucl Med 2010;51:193-197.
14. Tarkin JM, Joshi FR, Evans NR, Chowdhury MM, Figg NL, Shah AV, Starks LT, Martin-Garrido A, Manavaki R, Yu E, Kuc RE, Grassi L, Kreuzhuber R, Kostadima MA, Frontini M, Kirkpatrick PJ, Coughlin PA, Gopalan D, Fryer TD, Buscombe JR, Groves AM, Ouwehand WH, Bennett MR, Warburton EA, Davenport AP, Rudd JH. Detection of atherosclerotic inflammation by ^{68}Ga-DOTATATE PET compared to [^{18}F]FDG PET imaging. J Am Coll Cardiol 2017;69:1774-1791.
15. Høilund-Carlsen PF, Piri R, Constantinescu C, Iversen KK, Werner TJ, Sturek M, Alavi A, Gerke O. Atherosclerosis imaging with ^{18}F-sodium fluoride PET. Diagnostics (Basel) 2020;10:852.
16. Lee R, Seok JW. An Update on [18F] fluoride PET imaging for atherosclerotic disease. J Lipid Atheroscler 2020;9:349-361.
17. Li X, Samnick S, Lapa C, Israel I, Buck AK, Kreissl MC, Bauer W. 68Ga-DOTATATE PET/CT for the detection of inflammation of large arteries: correlation with18F-FDG, calcium burden and risk factors. EJNMMI Res 2012;2:52.
18. Amini A, Dehdar F, Jafari E, Gholamrezanezhad A, Assadi M. Somatostatin receptor scintigraphy in a patient with myocarditis. Mol Imaging Radionucl Ther 2021;30:50-53.
19. Leccisotti L, Nicoletti P, Cappiello C, Indovina L, Giordano A. PET imaging of vulnerable coronary artery plaques. Clin Transl Imaging 2019;7:267-284.
20. Fox K, Garcia MA, Ardissino D, Buszman P, Camici PG, Crea F, Daly C, De Backer G, Hjemdahl P, Lopez-Sendon J, Marco J, Morais J, Pepper J, Sechtem U, Simoons M, Thygesen K, Priori SG, Blanc JJ, Budaj A, Camm J, Dean V, Deckers J, Dickstein K, Lekakis J, McGregor K, Metra M, Morais J, Osterspey A, Tamargo J, Zamorano JL; Task Force on the Management of Stable Angina Pectoris of the European Society of Cardiology; ESC Committee for Practice Guidelines (CPG). Guidelines on the management of stable angina pectoris: executive summary: The Task Force on the Management of Stable Angina Pectoris of the European Society of Cardiology. Eur Heart J 2006;27:1341-1381.
21. Fihn SD, Gardin JM, Abrams J, Berra K, Blankenship JC, Dallas AP, Douglas PS, Foody JM, Gerber TC, Hinderliter AL, King SB 3rd, Kligfield PD, Krumholz HM, Kwong RY, Lim MJ, Linderbaum JA, Mack MJ, Munger MA, Prager RL, Sabik JF, Shaw LJ, Sikkema JD, Smith CR Jr, Smith SC Jr, Spertus JA, Williams SV; American College of Cardiology Foundation; American Heart Association Task Force on Practice Guidelines; American College of Physicians; American Association for Thoracic Surgery; Preventive Cardiovascular Nurses Association; Society for Cardiovascular Angiography and Interventions; Society of Thoracic Surgeons. 2012 ACCF/AHA/ACP/AATS/PCNA/SCAI/STS Guideline for the diagnosis and management of patients with stable ischemic heart disease: a report of the American College of Cardiology Foundation/American Heart Association Task Force on Practice Guidelines, and the American College of Physicians, American Association for Thoracic Surgery, Preventive Cardiovascular Nurses Association, Society for Cardiovascular Angiography and Interventions, and Society of Thoracic Surgeons. J Am Coll Cardiol 2012;60:44-164.
22. Tarkin JM, Joshi FR, Rudd JH. Advances in molecular imaging: plaque imaging. Current Cardiovascular Imaging Reports 2013;6:358-368.
23. Owen DR, Lindsay AC, Choudhury RP, Fayad ZA. Imaging of atherosclerosis. Annu Rev Med 2011;62:25-40.
24. Vancraeynest D, Pasquet A, Roelants V, Gerber BL, Vanoverschelde JL. Imaging the vulnerable plaque. J Am Coll Cardiol 2011;57:1961-1979.
25. Osborn EA, Jaffer FA. The year in molecular imaging. JACC Cardiovasc Imaging 2009;2:97-113.
26. Krishnan S, Otaki Y, Doris M, Slipczuk L, Arnson Y, Rubeaux M, Dey D, Slomka P, Berman DS, Tamarappoo B. Molecular imaging of vulnerable coronary plaque: a pathophysiologic perspective. J Nucl Med 2017;58:359-364.